

# Theoretical study of the SiO<sub>2</sub>/Si interface and its effect on energy band profile and MOSFET gate tunneling current

Zhu Huiwen(朱晖文)<sup>1,†</sup>, Liu Yongsong(刘咏松)<sup>1</sup>, Mao Lingfeng(毛凌峰)<sup>2</sup>, Shen Jingqin(沈静琴)<sup>1</sup>,  
Zhu Zhiyan(朱志艳)<sup>1</sup>, and Tang Weihua(唐为华)<sup>1</sup>

(1 Department of Physics, Center for Optoelectronics Materials and Devices, Zhejiang Sci-Tech University,  
Hangzhou 310018, China)

(2 School of Electronics & Information Engineering, Soochow University, Suzhou 215021, China)

**Abstract:** Two SiO<sub>2</sub>/Si interface structures, which are described by the double bonded model (DBM) and the bridge oxygen model (BOM), have been theoretically studied via first-principle calculations. First-principle simulations demonstrate that the width of the transition region for the interface structure described by DBM is larger than that for the interface structure described by BOM. Such a difference will result in a difference in the gate leakage current. Tunneling current calculation demonstrates that the SiO<sub>2</sub>/Si interface structure described by DBM leads to a larger gate leakage current.

**Key words:** interface; MOSFETs; gate tunneling current

**DOI:** 10.1088/1674-4926/31/8/082003

**PACC:** 7115M; 7340G; 7450

## 1. Introduction

The continuing growth of circuit density needs the dimensional scaling of MOSFETs, thus reducing the equivalent oxide thickness (EOT) of gate dielectric, which reaches values as small as several angstroms<sup>[1]</sup>. As a consequence, the interfacial transition layer between Si and its oxide has become a significant fraction of the total thickness, and its detailed physical properties have a strong impact on the device performance such as channel mobility, leakage current, time dependent dielectric breakdown, and hot-electron induced effects. Understanding the atomic scale structural and electronic properties of this interface is, therefore, of paramount importance for the progress of Si-based microelectronics. Despite decades of study, and the availability of a great deal of experimental information about the interface<sup>[2,3]</sup>, the precise bonding arrangement in the interface region remains unknown, partially because the oxide network is amorphous. Atomistic simulation treatment of the SiO<sub>2</sub>/Si interface is a technically challenging problem attempted by many groups using a variety of techniques. Several structural models of the SiO<sub>2</sub>/Si interface have been proposed<sup>[4-7]</sup>. However, there have been rather few theoretical studies on the effect of SiO<sub>2</sub>/Si interfaces on devices performance based on first principles calculations. In order to understand it, two interface models, the bridge-oxygen model (BOM)<sup>[8]</sup> and the double-bonded model (DBM)<sup>[9]</sup>, were chosen and calculated via first principles, and based on the calculations, their impact on the energy band profile and gate tunneling current was evaluated.

## 2. Calculation method

### 2.1. Model structures

It is well-known that SiO<sub>2</sub> is amorphous for the thermal ox-

idation grown gate dielectric in MOSFETs; however, the electronic properties of bulk SiO<sub>2</sub> crystals are still important in tunneling current analysis in the nanoscale oxide thickness according to Yamada *et al.*'s work<sup>[10]</sup>. The structural and electronic properties of many different crystalline forms of silicon dioxide such as amorphous SiO<sub>2</sub>,  $\alpha$ -quartz and  $\beta$ -cristobalite<sup>[11]</sup> have been studied by applying different theoretical and experimental methods<sup>[12-15]</sup>. However, there are no models which can precisely describe the overall atomic-scale properties of SiO<sub>2</sub>. A realistic model of SiO<sub>2</sub> is of primary importance when studying the SiO<sub>2</sub>/Si(100) interface. In the present work,  $\beta$ -cristobalite is a natural choice due to its structural simplicity<sup>[8,16-18]</sup>. The Si(100) surface was considered in this work because it is the most favored surface in MOSFET devices due to its low interface state density and correspondingly superior electrical characteristics.

Two simple-model structures for SiO<sub>2</sub>/Si interfaces, DBM (see Fig. 1(a)) and BOM (see Fig. 1(b)), were considered in this work. The modeled SiO<sub>2</sub>/Si supercell structures were constructed from 2 layers of crystalline diamond Si(100) and 2 layers of crystalline SiO<sub>2</sub> in the ideal  $\beta$ -cristobalite structure. The experimental lattice constants are 5.43 and 7.16 Å, respectively, and the lattice mismatch is 32%. The mismatch can be reduced by rotating the two SiO<sub>2</sub> unit cells by an angle of  $\pi/4$  so that the diagonal of the Si diamond structure approximately fits the cubic edge of the  $\beta$ -cristobalite unit cell. The superposition of the Si and SiO<sub>2</sub> layers produces dangling bonds on some of the interface Si atoms. These dangling bonds can be satisfied by adding a single O atom onto one of the Si atoms in the DBM. The resulting supercell has 73 atoms and dimensions 5.43 Å in the  $x$ - $y$  plane and 25.18 Å in the  $z$  direction. In the BOM, an O atom saturates two dangling bonds of two different Si atoms; this supercell contains 72 atoms. The Si-O-Si angle is 144° and the length of the interface Si-O bonds is 2.02 Å. No cell optimization of the models has been carried out.

† Corresponding author. Email: zhuhuiwen2008@gmail.com

Received 18 February 2010, revised manuscript received 29 March 2010

© 2010 Chinese Institute of Electronics

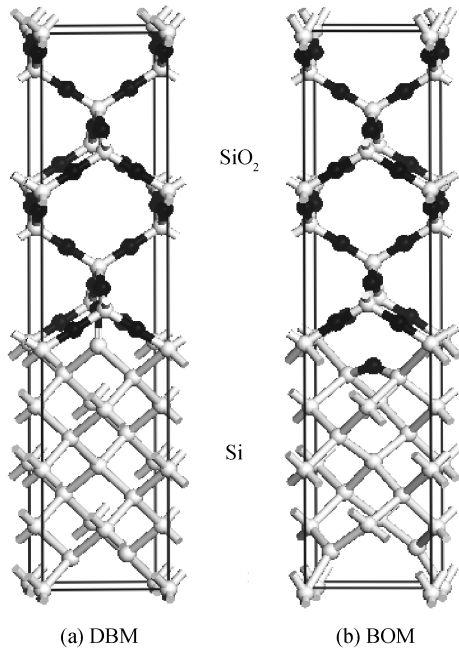


Fig. 1. Two SiO<sub>2</sub>/Si supercell models. (a) DBM, which contains 73 atoms (48 Si and 25 O). (b) BOM, which contains 72 atoms (47 Si and 25 O atoms). O: balls in black, and Si: balls in gray. Both unit cells are rectangular and of size 5.43 × 5.43 × 25.18 Å.

### 2.2. Macroscopic averaging potentials via first principles

The geometrical optimization and energy calculations were performed using the CASTEP program (Cambridge serial total energy package)<sup>[19]</sup>, which employs the plane pseudopotential method to calculate the total energy within the framework of the Kohn–Sham DFT. The calculations of electron-exchange associated items were carried out using the PW91 form of the GGA correction method. The Vanderbilt ultrasoft pseudopotentials were used, which allow numerically converged calculations at relatively low kinetic energy cutoffs of the plane wave basis. The Broyden, Fletcher, Goldfarb and Shanno (BFGS) algorithm was applied to optimize the model structures. Four *k*-points were taken in the Brillouin area, and the ground state energy was calculated with the Pulay density mixed method under the following conditions: the precision is 2.0 × 10<sup>-5</sup> eV per atom, the cutoff energy of the plane wave is 290 eV, 300 eV for BOM and DBM respectively.

Further, the valence band profiles were calculated using the average potential method<sup>[20]</sup>. The electrostatic potentials for the supercell were averaged in the *xy* plane; then, macroscopic averaging potentials were calculated in the *z* direction:

$$\overline{V(z)} = \frac{1}{t} \int_{z-t/2}^{z+t/2} V(z') dz', \quad (1)$$

where *V(z)* is the plane-averaged electrostatic potential, and *t* is the lattice periodicity along *z*.

### 2.3. Gate tunneling current calculation

As dielectric film thickness decreases, electrical transport due to direct and FN conduction dominates device characterization, and the transition region between SiO<sub>2</sub> and Si influences the Fowler–Nordheim (FN) tunneling and direct tunnel-

ing (DT) currents through the ultrathin oxide.

FN tunneling current through a triangular barrier can be written as<sup>[21,22]</sup>

$$J_{\text{FN}} = BF^2 \exp(-C/F), \quad (2)$$

where *F* is the electric field across the oxide, and *B* and *C* are constants and are given respectively by<sup>[23]</sup>

$$B = \frac{q^3 m}{16\pi^2 \hbar m_{\text{ox}}^* \phi_0}, \quad (3)$$

$$C = \frac{4}{3} \frac{(2m_{\text{ox}}^*)^{1/2}}{q\hbar} \phi_0^{3/2}, \quad (4)$$

where *m* is the free electron mass, *m<sub>ox</sub><sup>\*</sup>* is the effective mass of electron on the conduction band of SiO<sub>2</sub>, *ħ* is the reduced Planck's constant, and *φ<sub>0</sub>* is the barrier height (eV) between Si and SiO<sub>2</sub>.

The above FN equation for the tunneling current was derived using the Wentzel–Kramers–Brillouin (WKB)<sup>[24]</sup> approximation that the electron wave interference effect is neglected, the oxide layer is flat, and the barrier lowering by image force as well as the temperature were neglected.

Taking the transition region (width *d*) into account, the FN tunneling current through a triangular barrier can be rewritten as<sup>[25]</sup>

$$J = J_{\text{FN}} \exp \frac{2d\sqrt{2m_{\text{ox}}^* \phi_0}}{3\hbar} = B_1 F^2 \exp\left(-\frac{C}{F}\right), \quad (5)$$

where

$$B_1 = B \exp \frac{2d\sqrt{2m_{\text{ox}}^* \phi_0}}{3\hbar}. \quad (6)$$

The actual potential barrier deviates from the ideal triangular barrier because a transition region between Si and SiO<sub>2</sub> exists, and gradually changes from Si to SiO<sub>2</sub>. This actual barrier shape makes the FN tunneling current much higher compared with that of the ideal one. The transition region width has an exponential impact on the FN tunneling current from Eq. (5).

However, when the oxide layer becomes ultra-thin and the applied voltage is below the potential barrier height, the classical FN formula is not applicable. In this case, the direct tunneling current must be considered and it can be described as<sup>[26]</sup>

$$J_{\text{DT}} = \frac{B}{\left[1 - \left(1 - \frac{qV_{\text{ox}}}{\phi_0}\right)^{1/2}\right]^2} F^2 \times \exp\left(-\frac{C}{\frac{\phi_0^{3/2} - (\phi_0 - qV_{\text{ox}})^{3/2}}{\phi_0^{3/2}} F}\right). \quad (7)$$

Again, the band structure variations influence the direct tunneling current similar to that of FN tunneling current. The direct tunneling current will increase exponentially if the transition region extends more widely.

### 3. Results and discussion

#### 3.1. Energy band profile

At the SiO<sub>2</sub>/Si interface, the band changes continuously from Si to SiO<sub>2</sub> (Fig. 2). From Fig. 2 the interface region is roughly 5 Å for both models. Other groups have reported similar results for different SiO<sub>2</sub>/Si structures<sup>[27, 28]</sup>. The calculated interface region width is comparable with the experimental result<sup>[29]</sup>.

However, it is important to define the transition region in atomistic detail. A definition of the transition region has been provided by suboxide or partially oxidized Si atoms<sup>[30]</sup>. In the present study, another way was chosen. The coordinates in the *z* direction, corresponding to the band profile changes in a trend away from the averages and vice versa, were set as the interface region boundaries. For example, the band goes down away from its average at point *a* in Fig. 2, so the coordinate *z*<sub>1</sub> corresponding to point *a* can be set to a boundary for BOM interface structure. Similarly, the other boundary can be set at *z*<sub>2</sub>. This enabled us to easily evaluate the device performance such as calculating the gate FN tunneling current.

In the transition region, the band profiles behave differently for the two interface models. Firstly, the band of DBM is mostly higher than that of BOM. This can be easily understood by analyzing the charges of atoms in the transition region. All atoms distributed in the transition for DBM have more positive charges than those for BOM from the CASTEP calculations. Secondly, there is an obvious peak in the band of DBM, while there are no such peaks for BOM. The peak corresponds to the interface O atom double-bonded to Si. Due to a more positive chemical environment such as Si and O charges, it stands out from the band trend. The band profile is influenced by the interface structure<sup>[27]</sup>. Lastly, the band of BOM is closer to the average of the SiO<sub>2</sub> band than that of DBM. In other words, the transition region for BOM is thinner than that of DBM. This is because the BOM structure is less influenced by the interface O bridging two Si atoms, while the DBM structure is more influenced by the interface O double bonded to one atom; moreover, this interface O atom is near the SiO<sub>2</sub> layers from Fig. 1 and thus the band profile is closer to the SiO<sub>2</sub> band.

This transition region feature is supposed to influence the performance of devices consisting of SiO<sub>2</sub>/Si structures, e.g., gate FN tunneling current in MOSFETs.

#### 3.2. Gate tunneling current

As stated above, the band profile in the interface transition region varies mainly due to atomic scale interface structures. The band profiles deviate from the ideal abrupt barrier between Si and SiO<sub>2</sub>, and thus increase the FN tunneling current. Next, the FN tunneling currents through SiO<sub>2</sub> on Si with different interface structures were calculated and compared.

The transition region width was calculated according to the method discussed above. It is 3.2 and 5.6 nm respectively from Fig. 2. Other parameters used in this work are  $m_{ox}^* = 0.5 m$ ,  $\alpha = 1.4$ ,  $\phi_0 = 3.15$  eV and the thickness of SiO<sub>2</sub> is 1.62 nm. As mentioned earlier, the thickness of SiO<sub>2</sub> is larger than that of two layers of SiO<sub>2</sub> because the band profiles go deep in Si.

According to Eq. (6),  $B_1/B$  varies greatly with the two SiO<sub>2</sub>/Si interface models (Fig. 3), and it is 2.8 times larger for DBM. This means that the  $B_1$  factors are greatly increased for

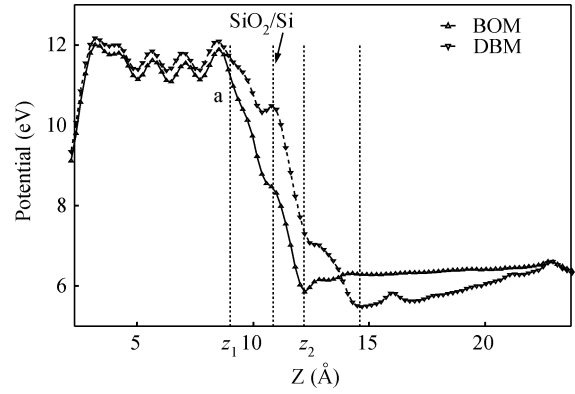


Fig. 2. Band profiles along the *z* direction for the SiO<sub>2</sub>/Si interface models DBM and BOM. Coordinates *z*<sub>1</sub>, *z*<sub>2</sub> correspond to transition region boundaries for BOM, the dotted line labeled with SiO<sub>2</sub>/Si means the original SiO<sub>2</sub>/Si interface as the models set.

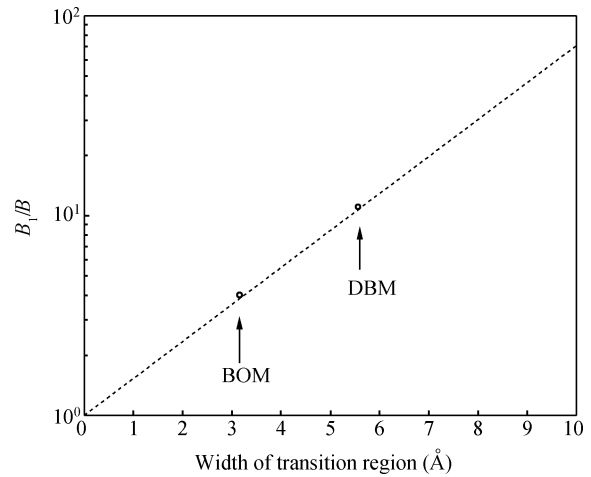


Fig. 3.  $B_1/B$  comparison for SiO<sub>2</sub>/Si interface structures: DBM and BOM.

Table 1. FN tunneling current (A/cm<sup>-2</sup>) versus interface structures under applied voltages.

Voltage (Interface)	1	2
Ideal barrier	$4.3 \times 10^{-12}$	$2.0 \times 10^{-5}$
BOM	$1.7 \times 10^{-11}$	$7.9 \times 10^{-5}$
DBM	$2.9 \times 10^{-11}$	$1.4 \times 10^{-4}$

both DBM and BOM SiO<sub>2</sub>/Si structures, compared with that of the ideal SiO<sub>2</sub>/Si structure because there are transition regions for the two models, and the barrier is changed.

The FN tunneling currents for ideal, BOM and DBM interface structures were calculated (Fig. 4). For the DBM and BOM SiO<sub>2</sub>/Si interface structures, the tunneling currents are larger than that of the ideal barrier SiO<sub>2</sub>/Si interface structure. One can have a rough image from Table 1. Obviously the DBM interface structure has the most impact on the gate FN tunneling current.

Furthermore, the calculated direct tunneling current for the BOM interface structure is roughly 3 times larger than that of the ideal barrier interface structure, while the direct tunneling current for the DBM interface structure is roughly one order

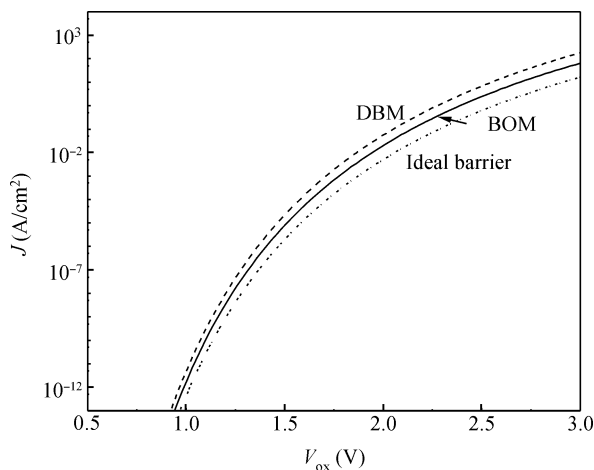


Fig. 4. Effect of SiO<sub>2</sub>/Si interfaces on FN tunneling current under different applied voltages across the oxide.

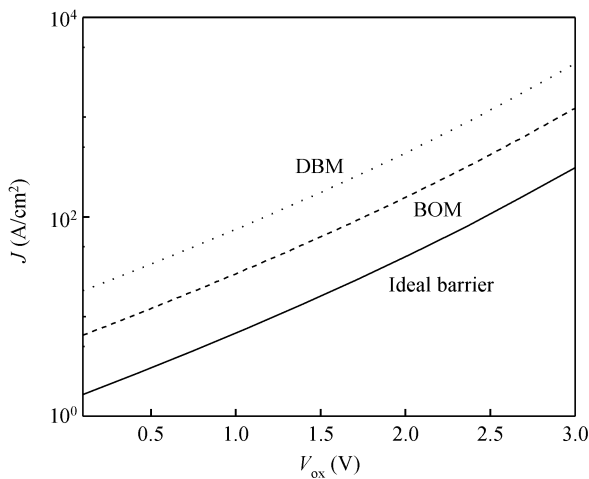


Fig. 5. Effect of SiO<sub>2</sub>/Si interfaces on direct tunneling current under different applied voltages across the oxide.

larger (Fig. 5). The energy band for the DBM interface structure extends more widely in the transition region, and it thus greatly increases the direct tunneling current. Compared with the calculated FN tunneling currents, the direct tunneling currents are larger and are strongly affected by the SiO<sub>2</sub>/Si interface structures.

The gate tunneling current depends on the SiO<sub>2</sub>/Si interface structure because the barrier varies with SiO<sub>2</sub>/Si interfaces. This tunneling current affects the device performance, and increases the power dissipation of the circuits. As high dielectric constant dielectrics are integrated into the devices, it is observed that an interfacial oxide layer exists between the high dielectric constant material and Si substrate<sup>[31]</sup>, and the interface issue between Si and its oxides is still a primary challenge for Si-based technology.

#### 4. Conclusion

The SiO<sub>2</sub>/Si interface is of primary importance for Si-based semiconductor devices. By considering two interface models, the present work has investigated the interface band profile and

its impact on gate tunneling current via first principle calculations. The results show how the band profile varies with interface structures for the chemical environment variation in the transition region. The band profile of the DBM SiO<sub>2</sub>/Si interface is higher and extends more widely than that of the BOM SiO<sub>2</sub>/Si interface. Furthermore, the gate FN and direct tunneling current are exponentially increased because a transition region exists between SiO<sub>2</sub>/Si, and it is increased more for the DBM SiO<sub>2</sub>/Si interface. The SiO<sub>2</sub>/Si interface greatly impacts the MOSFET performance, which needs to be extensively evaluated<sup>[32]</sup>.

#### Acknowledgement

One of the authors would like to thank Prof. Liu Xiaoyan from Peking University for her helpful advice.

#### References

- [1] ITRS <http://www.itrs.net/>
- [2] Hattori T. Chemical structures of the SiO<sub>2</sub>/Si interface. *Critical Reviews in Solid State and Materials Sciences*, 1995, 20(4): 339
- [3] Jang H J, Appelbaum I. Spin polarized electron transport near the Si/SiO<sub>2</sub> interface. *Phys Rev Lett*, 2009, 103(11): 117202
- [4] Watanabe T, Tatsumura K, Ohdomari I. SiO<sub>2</sub>/Si interface structure and its formation studied by large-scale molecular dynamics simulation. *Appl Surf Sci*, 2004, 237(1–4): 125
- [5] Tu Y, Tersoff J. Structure and energetics of the Si–SiO<sub>2</sub> interface. *Phys Rev Lett*, 2000, 84(19): 4393
- [6] Ng K O, Vanderbilt D. Structure and oxidation kinetics of the Si(100)–SiO<sub>2</sub> interface. *Phys Rev B*, 1999, 59: 10132
- [7] Van Ginhoven R M, Hjalmarson H P, Edwards A H, et al. Hydrogen release in SiO<sub>2</sub>: source sites and release mechanisms. *Nuclear Instruments and Methods in Physics Research Section B: Beam Interactions with Materials and Atoms*, 2006, 250(1/2): 274
- [8] Carrier P, Lewis L J, Dharma-Wardana M W C. Electron confinement and optical enhancement in Si/SiO<sub>2</sub> superlattices. *Phys Rev B*, 2001, 64: 195330
- [9] Herman F, Batra I P. The physics of SiO<sub>2</sub> and its interfaces. In: Pantelides S T, ed. Oxford: Pergamon, 1978
- [10] Yamada Y, Tsuchiya H, Ogawa M. A first principles study on tunneling current through Si/SiO<sub>2</sub>/Si structures. *J Appl Phys*, 2009, 105(8): 083702
- [11] Giustino F, Umari P, Pasquarello A. Dielectric effect of a thin SiO<sub>2</sub> interlayer at the interface between silicon and high-*k* oxides. *Microelectron Eng*, 2004, 72(1–4): 299
- [12] Liu F, Garofalini S H, King-Smith R D, et al. First-principles studies on structural properties of beta-cristobalite. *Phys Rev Lett*, 1993, 70: 2750
- [13] Swainson I P, Dove M T. Comment on “first-principles studies on structural properties of beta-cristobalite”. *Phys Rev Lett*, 1993, 71: 3610
- [14] Teter D M, Gibbs G V, Boisen M B, et al. First-principles study of several hypothetical silica framework structures. *Phys Rev B*, 1995, 52: 8064
- [15] Mauri F, Pasquarello A, Pfrommer B G, et al. Si–O–Si bond-angle distribution in vitreous silica from first-principles <sup>29</sup>Si NMR analysis. *Phys Rev B*, 2000, 62: R4786
- [16] Himpsel F J, McFeely F R, Taleb-Ibrahimi A, et al. Microscopic structure of the SiO<sub>2</sub>/Si interface. *Phys Rev B*, 1988, 38: 6084
- [17] Capron N, Boureau G, Pasturel A, et al. Thermodynamic properties of the Si–SiO<sub>2</sub> system. *The Journal of Chemical Physics*, 2002, 117(4): 1843

- [18] Hane M, Miyamoto Y, Oshiyama A. Atomic and electronic structures of an interface between silicon and beta-cristobalite. *Phys Rev B*, 1990, 41: 12637
- [19] Segall M D, Lindan P J D, Probert M J, et al. First-principles simulation: ideas, illustrations and the CASTEP code. *Journal of Physics: Condensed Matter*, 2002, 14(11): 2717
- [20] Van de Walle C G, Martin R M. Theoretical study of band offsets at semiconductor interfaces. *Phys Rev B*, 1987, 35: 8154
- [21] Lenzlinger M, Snow E H. Fowler–Nordheim tunneling into thermally grown SiO<sub>2</sub>. *J Appl Phys*, 1969, 40(1): 278
- [22] Weinberg Z A. Tunneling of electrons from Si into thermally grown SiO<sub>2</sub>. *Solid-State Electron*, 1977, 20(1): 11
- [23] Weinberg Z A. On tunneling in metal–oxide–silicon structures. *J Appl Phys*, 1982, 53(7): 5052
- [24] Bohm D. *Quantum theory*. Englewood Cliffs, NJ: Prentice Hall Inc, 1963
- [25] Mao Lingfeng, Tan Changhua, Xu Mingzhen. Estimate of width of transition region of barrier for thin film insulator MOS structure using Fowler–Nordheim tunneling current. *Chinese Journal of Semiconductors*, 2001, 22(2): 228
- [26] Wei J, Mao L, Xu M, et al. Direct tunneling relaxation spectroscopy in ultra-thin gate oxide MOS structures. *Solid-State Electron*, 2000, 44(11): 2021
- [27] Yamashita Y, Yamamoto S, Mukai K, et al. Direct observation of site-specific valence electronic structure at the SiO<sub>2</sub>/Si interface. *Phys Rev B*, 2006, 73: 045336
- [28] Alkauskas A, Broqvist P, Devynck F, et al. Band offsets at semiconductor–oxide interfaces from hybrid density-functional calculations. *Phys Rev Lett*, 2008, 101: 106802
- [29] Kimura K, Nakajima K. Compositional transition layer in SiO<sub>2</sub>/Si interface observed by high-resolution RBS. *Appl Surf Sci*, 2003, 216(1–4): 283
- [30] Blaha P, Schwarz K, Sorantin S B, et al. Full-potential, linearized augmented plane wave programs for crystalline systems. *Comput Phys Commun*, 1990, 59(2): 399
- [31] Först C J, Ashman C R, Schwarz K, et al. The interface between silicon and a high-*k* oxide. *Nature*, 2004, 427(6969): 53
- [32] Orellana W, da Silva A J R, Fazzio A. Oxidation at the Si/SiO<sub>2</sub> interface: influence of the spin degree of freedom. *Phys Rev Lett*, 2003, 90: 016103